Proceedings – 23rd Annual Conference – IEEE/EMBS Oct.25-28, 2001, Istanbul, TURKEY

MEDIAL AXIS REGISTRATION OF SUPINE AND PRONE CT COLONOGRAPHY DATA

B. Acar[1], S. Napel[1], D.S. Paik[1], P. Li[1], J. Yee[2], R.B. Jeffrey, Jr.[1], C.F. Beaulieu[1]
[1]Department of Radiology, LUCAS MRS Center, 3D Lab., Stanford University, Stanford, CA, USA
[2]San Francisco VA Medical Center, UCSF, San Francisco, CA, USA

Abstract- **Computed Tomographic Colonography (CTC) is a minimally invasive method that allows the examination of the colon wall from the source CT sections or in a virtual environment. The primary goal of CTC is the detection of colonic polyps. There are typically two data sets recorded in supine and prone positions. An important step in polyp detection is the anatomical registration of these datasets. We developed and experimentally validated a method to register complementary supine and prone CTC datasets anatomically, using linear stretching/shrinking operations on the medial axis colonic path based on the relative path geometries. To compare improvement in spatial registration of supine and prone datasets, a radiologist determined 5 unique reference points (RP) in the registered and unregistered datasets from each of 5 patients by viewing supine and prone data simultaneously. Initial results suggest that our algorithm is capable of registering supine and prone CTC data anatomically within an approximate range of ±13.2mm, which corresponds to 0.8% error with respect to the average colon length.**

Keywords **- CTC, Virtual colonography, registering prone and supine data for CTC, data fusion, anatomical data registration**

I. INTRODUCTION

Computed Tomographic Colonography (CTC) is a minimally invasive method for the examination of the colon using spiral/helical CT volume data [1]. The standard imaging process consists of colon cleansing and air-insufflation, followed by the CT imaging of the abdomen while the patient is in the supine position. However, insufficient cleansing and air-insufflation often cause some parts of the colon wall to be covered with water [3-5]. Furthermore, retained solid fecal material can mimic a polyp in CT images [2]. These limitations are largely overcome by imaging the colon a second time with the patient prone. The radiologists then compare the two sets of images simultaneously to assess for movement of feces and to examine surfaces hidden in supine position. This requires careful anatomic alignment between the two data sets. However, as the patients change position, their colons deform and may stretch or shrink in length. Currently, anatomic matching the two data sets is tedious and time consuming.

In this study, we developed and evaluated a fully automatic algorithm for the registration of prone and supine CTC data. Such an algorithm should improve the radiologist's overall interpretation efficiency as well as provide a basis for combining supine/prone Computer-Aided Detection (CAD) results automatically. Our approach is based on determining relatively stationary points along the medial axis pathsof the colon (*path*) for both positions, then matching these points by simple stretching and/or shrinking of either the supine or prone path. The algorithm was evaluated on a set of 5 patients, based on the average distance along the path between two anatomically identical points in prone and supine data.

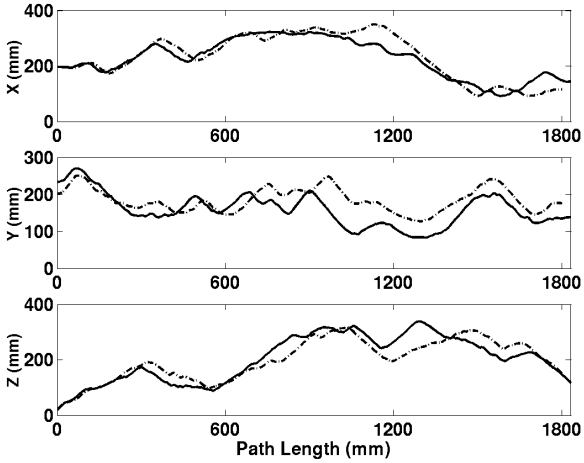

Figure 1. X, Y and Z coordinates along the supine path (Solid lines) and prone path (Dashed lines). Note that the supine path is longer than the prone path.

II. METHODOLOGY

A. Background

Colon wall segmentations for both the 3D prone (pCT) and supine (sCT) CT data were done using a fixed intensity threshold of –700 HU. The paths were computed using custom software and sampled at 1mm intervals [6]. The x, y and z coordinates of the path points were used as the inputs to the registration algorithm. As a convention, the $+z$ axis is from feet to head, the $+x$ axis is from the left side of the patient to the right side and the $+y$ axis from posterior to anterior. Distances along the path and the coordinates are referenced to the initial path point at the anus.

The path coordinates of sCT (x_s, y_s, z_s) and pCT (x_p, y_p, z_p) are functions of the distance along the path, d. Fig. 1 shows these six functions for a single patient. An important observation at this point is that x_s, y_s, z_s resemble x_p, y_p, z_p, respectively in terms of their morphologies. In what follows, we focus on the z axis for the sake of simplicity, though the algorithm can be similarly applied to any individual (or combination of) axis (axes). This latter approach is addressed later.

The morphological similarity between z_s and z_p can be seen as a similarity between the number of local extrema (LoP) and their order in terms of their z values. In other words, if we sort the LoP's with respect to their z values, the LoP's of z_s and z_p with equal or close indices are more likely to correspond to the same anatomical points along the paths. In anatomic terms, LoP's correspond to the deflection

Report Documentation Page

Report Date	Report Type	Dates Covered (from... to)
25OCT2001	N/A	-

Title and Subtitle Medial Axis Registration of Supine and Prone CT Colonography Data	**Contract Number**
	Grant Number
	Program Element Number
Author(s)	**Project Number**
	Task Number
	Work Unit Number
Performing Organization Name(s) and Address(es) Department of Radiology, LUCAS MRS Center, 3D Lab., Stanford University, Stanford, CA	**Performing Organization Report Number**
Sponsoring/Monitoring Agency Name(s) and Address(es) US Army Research, Development & Standardization Group (UK) PSC 802 Box 15 FPO AE 09499-1500	**Sponsor/Monitor's Acronym(s)**
	Sponsor/Monitor's Report Number(s)

Distribution/Availability Statement
Approved for public release, distribution unlimited

Supplementary Notes
Papers from the 23rd Annual International Conference of the IEEE Engineering in Medicine and Biology Society, 25-28 Oct 2001, held in Istanbul, Turkey. See also ADM001351 for entire conference on cd-rom.

Abstract

Subject Terms

Report Classification unclassified	**Classification of this page** unclassified
Classification of Abstract unclassified	**Limitation of Abstract** UU

Number of Pages
4

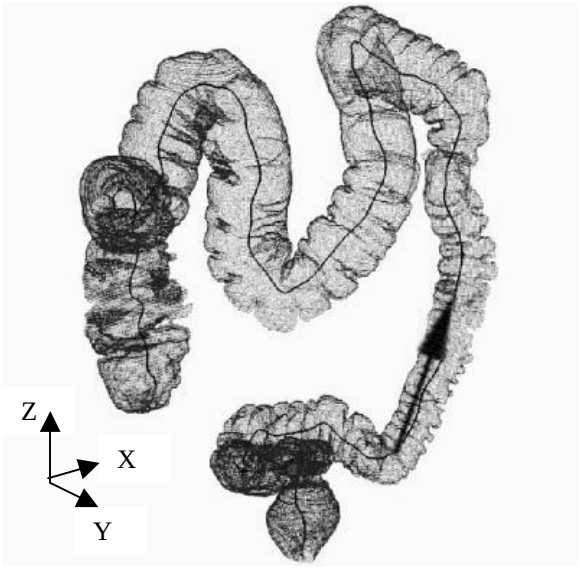

Figure 2. The colon wall extracted from 3D CT data by simple thresholding and the central axis path extending from the anus to the cecum.

points along the path. Despite of the fact that these deflection points move within the 3D volume (the patients' abdomen), they remain to be deflection points with small shifts in their locations with respect to d. Furthermore, LoP's with high z values are the points furthest away from the anus. Anatomically, these points typically correspond with the hepatic and splenic flexures, locations that are relatively fixed in location. These flexures mark the beginning and ending of the much more mobile transverse colon (see Fig. 2). (LoP's along the other axes correspond with different anatomical points.) Our method is based on coupling LoP's of z_s and z_p and matching their positions with respect to d by simple segmental stretching and/or shrinking of one of the two paths.

B. Algorithm

The first step is baseline adjustment. We assume that the beginning and the ending points of the two paths (spPt and prPt) correspond to the same anatomical points, the anus and the tip of the cecum. Let the path length functions of spPt and prPt be $D_s(i) = i, i \in [1, N_s]$ and $D_p(i) = i, i \in [1, N_p]$, respectively. A linear transformation, T, is applied such that

$$D_p(1) = \hat{D}_s(1) = T(D_s(1)) \quad (1)$$

$$D_p(N_p) = \hat{D}_s(N_s) = T(D_s(N_s)) \quad (2)$$

This is equivalent to taking the first and the last points of the two paths as two pairs of coupled LoP's of spPt and prPt and matching them with respect to d. The z values along the spPt are also changed linearly such that $z_s(1) = z_p(1)$ and $z_s(N_s) = z_p(N_p)$. Note that the linear transformation, T, is the mapping between spPt and prPt. It will be modified

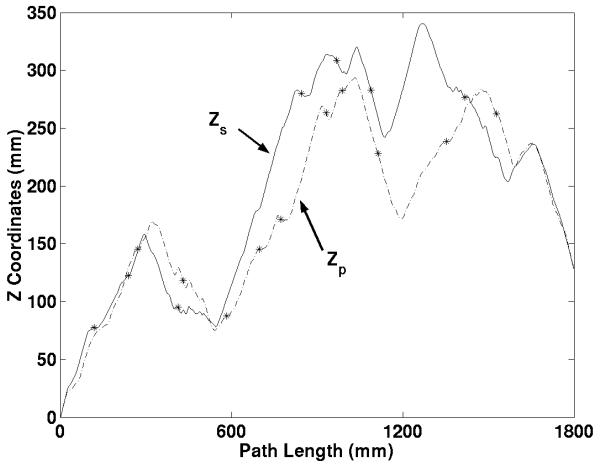

Figure 3. Z coordinates versus path length of supine (Z_S) and prone (Z_p) data after baseline adjustment. The * indicate the LoP_s's and LoP_p's

in the subsequent steps in a nonlinear fashion to yield to final piecewise linear mapping function.

The second step is to determine the LoP's. The local extrema of $z_s(\hat{D}_s)$ and $z_p(D_p)$ are determined using numerical derivation and neighboring extrema are clustered such that the minimum distance along the path between two consecutive clusters is 15mm. The mean location along the path and the mean z value for spPt and prPt (LoP_s and LoP_p respectively) are used. LoP_s's and LoP_p's, thus found, are ordered with respect to their z values and indexed. Fig. 3 shows the LoP_s's and LoP_p's for z_s and z_p.

The next step is to find the LoP_s,-LoP_p pair most likely to correspond to the same anatomical point. The decision criteria is based on the differences between their z values and their locations along the path:

If

$$i, j \in \{1,2\} \quad and \quad (3)$$

$$\left| \hat{D}_s\left(LoP\_s(i)\right) - D_p\left(LoP\_p(j)\right) \right| < 100mm \quad (4)$$

$$K < \hat{D}_s, D_p < L \quad (5)$$

where i and j are indices assigned to LoP's in the region of interest (ROI, Region Of Interest, is defined by (5)) only, with respect to their z values. Condition (3) forces the algorithm to match LoP's starting from the ones furthest away from the anus, i.e., the ones most likely to correspond to anatomical landmarks (like the hepatic and splenic flexures). Condition (4) is a constraint on the maximum stretching/shrinking allowed. Condition (5) defines the boundaries of ROI on which the registration is applied. Initially, $K = D_p(N_p) = \hat{D}_s(N_s)$ and

1.Do baseline correction
2.Find LoP's
3.Initialize recursion_level=0 and K *and* L *to set ROI*
4.Sort and index LoP's in ROI
5.If recursion_level<max_recursion_level
5.1.Match a pair of LoP_s and LoP_p based on (3),(4),(5)
5.2.If no match, go to step 6
5.3.Update $\hat{D}_s$ *by applying* $T(\ )$, *as in (6)*
5.4.Increase recursion_level by 1
5.5. $K_0 = K, \quad L_0 = L$
5.6.Set $K = \hat{D}_s(LoP\_s(i)) = D_p(LoP\_p(j))$
5.7.Go to step 4 (Process right-hand side)
5.8.Set
$K = K_0, L = \hat{D}_s(LoP\_s(i)) = D_p(LoP\_p(j))$
5.9.Go to step 4 (Process left-hand side)
6.Output $\hat{D}_s$.

Figure 4. The recursive registration algorithm

$L = D_p(1) = \hat{D}_s(1)$. Then a linear stretching/shrinking operation is applied to $\hat{D}_s$ such that

$$T(\hat{D}_s(LoP\_s(i))) = D_p(LoP\_p(j)) \qquad (6)$$

The algorithm matches the right- and left- hand sides of the matched point recursively, for a pre-specified level of recursions or until it could not find any pair of LoP's that satisfy the above criteria. Fig. 4 summarizes the algorithm.

C. Iteration and Parameters

The algorithm described above for z axis, can be similarly applied to x and y axes exactly in the same way. The order in which the axes are considered is a parameter of the algorithm. The entire process can be iterated until it converges to a final $\hat{D}_s$ or for a pre-specified number of iterations.

Table 1 provides a list of the parameters of the algorithm. The analysis in the following section will be based on variations of these parameters.

D. Initial Clinical Evaluation

We evaluated the improvement in spatial registration of identical anatomy in supine and prone data sets from 5 patients (all male, age 64-77, mean age 70). CT data were acquired in each position after colon cleansing and air-insufflation, using a single-detector CT system (GE Medical Systems, Milwaukee, WI). Imaging parameters were 3mm collimation, pitch 1.5-2.0, 1.5mm reconstruction interval,

TABLE I
THE PARAMETERS OF THE ALGORITH

Parameter	Definition
MaxIter	Maximum number of iterations
Axes	Axes to be used and their order
MaxRec	Maximum recursion level
ClstDLoP	Minimum d between neighboring groups of local extrema
MaxDLoP	Maximum d between matched LoP_s and LoP_p. Different for x, y, z.

120 KVp, 200 MAs. A radiologist determined 5 unique reference points (RP) in each of 5 patients by viewing supine and prone data simultaneously. Reference points included polyps, diverticulae, unique haustral folds, or the ileocecal valve. We computed the distance in terms of d between anatomically identical RPs in supine and prone data both before and after path registration. The change in the mean distance between pre- and post-registration RP positions was computed as a percentage of the pre-registration distance. In the following, we report the mean of these percentage values (Δd) over all patients in the dataset. Δd provides an overall understanding of the performance of the algorithm and is used to assess different parameter values. The parameter ranges used are: MaxIter=[1 2], Axes=[{ z }, { z, x, y }, { z, x }, { z, y }], MaxRec=[1 2 3], ClstDLoP=[10 15 … 40], MaxDLoP=[(42,42,70), (48,48,80), …, (72,72,120)]. Each parameter was evaluated separately, keeping the others constant.

III. RESULTS

To assess each parameter, we assigned a value to that parameter from the sets given above, held it constant and computed Δd for all combinations of the remaining parameters. This resulted in 504, 252, 336, 144, and 168 Δd's for a single value of MaxIter, Axes, MaxRec, ClstDLoP, and MaxDLoP, respectively. The respective mean values of Δd's were [-52.3%, -52.5%], [-52.4%, -52.0%, -53.3%, -52.0%], [-52.5%, -52.4%, -52.4%], [-35.6%, -56.4%, -53.8%, -51.2%, -55.3%, -57.2%, -57.5%], [-44.4%, -47.5%, -47.3%, -59.5%, -60.4%, -55.5%]. Note that more negative the mean Δd, the better registered the RPs. We assessed for significant differences between Δd's between values of a single parameter with the Student's t-test. All p-values were less than 0.05 except in the following cases: *(i)* between different MaxRec values and, *(ii)* between using axes { z }, { z, x, y } and { z, y }.

Based on these results, we decided to use the following set of parameters for path registration in this data set, with our rationale explained following each parameter: *i)* MaxIter=1: The difference in mean Δd's was small. *ii)* Axes={ z, x }: There is a significant improvement of approximately 1% with respect to the other choices. *iii)* MaxRec=1: Higher values did not improve the performance significantly. *iv)* ClstDLoP=15: This corresponded with a local minimum

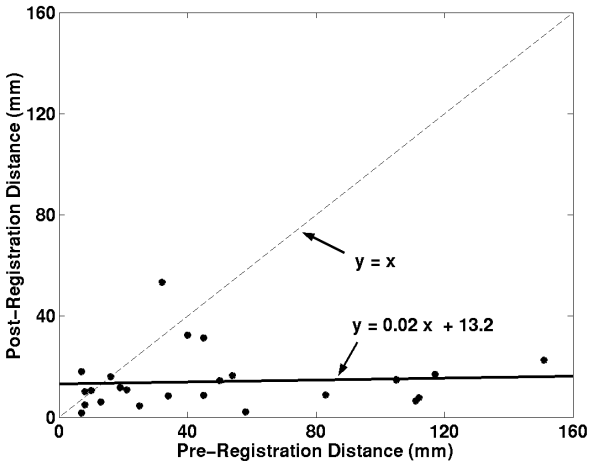

Figure 5. Pre- and post-registration distances along the path between 25 pairs of RPs in supine and prone CTC data.

significantly different that the others. The lower mean Δd values for ClstDLoP=35 and 40 were not chosen as they did not represent a local optimum point and because large ClstDLoP values result in large clusters that may localize LoP's with sufficient resolution. *v)* MaxDLoP=[66 66 100]: This was a local minimum significantly different from the other values.

The mean (±s.d.) Δd with the optimal parameter settings was (-67.0±25.8)%. The mean (±s.d.) pre-registration distance of 51.0±42.8mm was decreased to 14.2±11.3mm. The maximum pre-registration distance of 151.0mm was decreased to 22.5mm. Fig.5 summarizes the results. The point-to-point distance was increased by registration in only 4 out of 25 RPs (5 RP per patient) (from 14.3±11.9mm to 23.0±20.5mm). These are the points above the y=x line in Fig. 5.

IV. Discussion

Fig. 5 shows every RP in the dataset with the line fitted in the least-squares sense. It suggests that our method can register any two points along the colon path with an approximate average error of 14.2mm, irrespective of the pre-registration distance between these points.

These initial results support the validity of our assumption that the colon undergoes apparent linear stretching and shrinking with changes in patient position. There may also occur twisting of the colon around the colon path, though we do not yet evaluate for this effect. Such evaluation will require a more detailed point-wise registration of the colon walls in different positions.

One of our results presented above show that the larger the variation in the coordinate values, the more the information content. In support of this, we found that the z and x axes are the most important axes. This makes sense as the colon more or less lies on the (z, x) plane (coronal plane).

V. Conclusion

We have developed and experimentally evaluated an algorithm to register supine and prone CTC data with respect to positions along the central path of the colon. Possible second order effects such as twisting of the colon wall around the path is the subject of future research. These initial results suggest that our algorithm is capable of registering supine and prone CTC data anatomically within an approximate average error of 14.2mm, which corresponds to 0.9% error with respect to the average colon length. This is a significant improvement over the pre-registration distance of 51mm. From a clinical perspective, this suggests that a given anatomic point in a complementary supine or prone dataset can be identified with a ~3 cm zone compared with a ~10 cm range using non-registered data. With further validation and refinement, our path-registration algorithm will allow for more efficient simultaneous data viewing by radiologists and enable accurate anatomic correlation of computer-aided detection results between patient positions.

References

[1] D.J. Vining, "Virtual colonoscopy," *Gastrointest. Endosc. Clin. N. Am.*, vol. 7(2), pp. 285-291, 1997.

[2] J.G. Fletcher, C.D. Johnson, R.L. MacCarty, T.J. Welch, J.E. Reed, A.K. Hara, "CT colonography: potential pitfalls and problem-solving techniques," *Am J Roentgenol*, vol. 172(5), pp. 1271-1278, 1999. (With comments in *Am J Roentgenol*, vol. 172(5), pp. 1179, 1999)

[3] S.C. Chen, D.S. Lu, J.R. Hecht, B.M. Kadell, "CT colonography: value of scanning in both the supine and prone positions," *Am J Roentgenol*, vol. 172(3), pp. 595-599, 1999.

[4] J.G. Fletcher, C.D. Johnson, T.J. Welch, R.L. MacCarty, D.A. Ahlquist, J.E. Reed, W.S. Harmsen, L.A. Wilson, "Optimization of CT colonography technique: prospective trial in 180 patients," *Radiology*, vol. 216(3), pp. 704-711, 2000.

[5] J. Yee, R.K. Hung, G.A. Akerkar, S.D. Wall, "The usefulness of glucagon hydrochloride for colonic distention in CT colonography," *Am J Roentgenol*, vol. 173(1), pp. 169-172, 1999.

[6] D.S. Paik, C.F. Beaulieu, R.B. Jeffrey, G.D. Rubin, S. Napel, "Automated flight path planning for virtual endoscopy," *Medical Physics*, vol. 25(5), pp. 629-637, May 1998.